

MicroAUNet: Boundary-Enhanced Multi-scale Fusion with Knowledge Distillation for Colonoscopy Polyp Image Segmentation

Ziyi Wang¹, Yuanmei Zhang¹, Dorna Esrafilzadeh², Ali R. Jalili² and Suncheng Xiang^{1*}

¹Shanghai Jiao Tong University, Shanghai, 200240, China.

²University of New South Wales (UNSW), Sydney, 2052, Australia.

*Corresponding author(s). E-mail(s):

xiangsuncheng17@sjtu.edu.cn;

Contributing authors: chloewangzy@163.com;

yuan-0102@alumni.sjtu.edu.cn; d.esrafilzadeh@unsw.edu.au;

ali.jalili@unsw.edu.au;

Abstract

Early and accurate segmentation of colorectal polyps is critical for reducing colorectal cancer mortality, which has been extensively explored by academia and industry. However, current deep learning-based polyp segmentation models either compromise clinical decision-making by providing ambiguous polyp margins in segmentation outputs or rely on heavy architectures with high computational complexity, resulting in insufficient inference speeds for real-time colorectal endoscopic applications. To address this problem, we propose MicroAUNet, a light-weighted attention-based segmentation network that combines depthwise-separable dilated convolutions with a single-path, parameter-shared channel–spatial attention block to strengthen multi-scale boundary features. On the basis of it, a progressive two-stage knowledge-distillation scheme is introduced to transfer semantic and boundary cues from a high-capacity teacher. Extensive experiments on benchmarks also demonstrate the state-of-the-art accuracy under extremely low model complexity, indicating that MicroAUNet is suitable for real-time clinical polyp segmentation. The code is publicly available at <https://github.com/JeremyXSC/MicroAUNet>.

Keywords: Colonoscopic Polyp Identification, light-weighted network, Attention mechanism, Knowledge distillation

1 Introduction

Colorectal cancer (CRC) remains one of the most prevalent and deadly malignancies worldwide (Mei et al, 2025; Qayoom et al, 2025). Early detection and removal of precancerous polyps during colonoscopy have proven to be the most effective strategy for reducing CRC incidence and mortality. However, traditional colonoscopy heavily relies on physician expertise, facing challenges such as a high miss rate (approximately 20-30%) and significant operational burden due to visual fatigue and difficulties in detecting small or flat polyps (Akgöl et al, 2025; Sabri et al, 2025). Deep learning-based computer-aided systems offer a promising solution to improve polyp detection rates, wherein accurate polyp image segmentation serves as the foundational step for subsequent analysis and diagnosis (Si et al, 2023). Despite these advances, several challenges persist in clinical scenarios.

Deep-learning-based polyp segmentation models still suffer from two fundamental limitations. First, precise boundary delineation remains challenging due to complex background interference and morphological diversity among heterogeneous image quality. This limitation may compromise clinical decision-making by providing ambiguous polyp margins in segmentation outputs. Second, many high-performing models rely on heavy architectures with high computational complexity and extensive parameterisation, resulting in insufficient inference speeds for real-time colorectal endoscopic applications. Consequently, developing a segmentation network that simultaneously achieves high boundary precision and computational efficiency remains an open research challenge. An overview of the motivation and design logic of our proposed framework is illustrated in Figure 1, which highlights the key challenges in existing segmentation models and the corresponding solutions adopted by MicroAUNet.

Our proposed MicroAUNet addresses these limitations through a novel co-design that introduces a boundary-aware module to capture fine-grained details under complex backgrounds while employing a highly efficient single-path architecture with progressive distillation. This approach enables precise real-time segmentation that was previously unattainable by light-weighted models.

The main contributions of this paper can be summarised as follows.

- We propose a light-weighted attention-based segmentation network named MicroAUNet, which combines depthwise separable dilated convolutions with a shared channel-spatial attention mechanism to improve boundary extraction and adaptability to polyps of diverse morphologies.

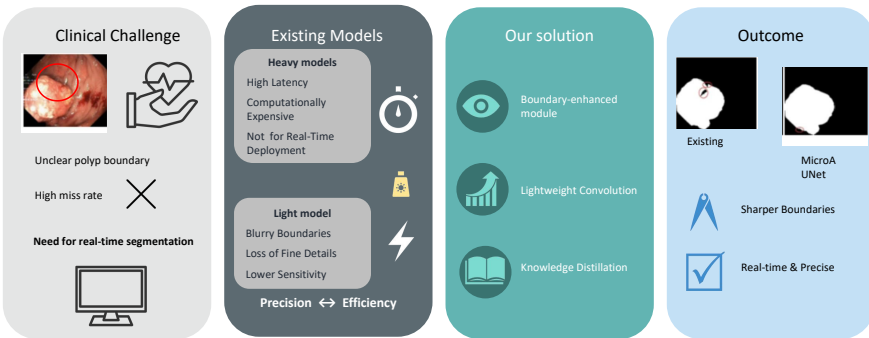


Fig. 1 Motivation and overall design concept of the proposed MicroAUNet framework. It illustrates the limitations of existing polyp segmentation models—blurred boundaries and high computational costs, and this paper integrates boundary enhancement, light-weighted attention, and knowledge distillation to overcome these challenges.

- A progressive two-stage knowledge distillation mechanism is introduced to transfer semantic and boundary knowledge from a teacher model, enabling robust light-weighted learning with minimal computational cost.
- Comprehensive validation on public datasets demonstrates the superiority of the proposed model in both segmentation accuracy and inference efficiency compared to existing state-of-the-art methods, highlighting its potential for clinical application.

The remainder of this paper is structured as follows. Section 2 reviews related works on CNN-based, light-weighted, and attention-driven segmentation networks. In Section 3, the details of the proposed MicroAUNet with reshaped blocks and a light-weighted structure are presented. Extensive evaluations compared with state-of-the-art methods and comprehensive analyses of the proposed approach are reported in Section 4. Finally, Section 5 presents the conclusion and discussion of future work.

2 Related Work

2.1 CNN-based Methods

Early research on colonoscopy polyp segmentation primarily focused on convolutional neural networks (CNNs), which significantly improved segmentation accuracy by effectively capturing multi-scale features through local connectivity and weight-sharing mechanisms. The fully convolutional network (FCN) (Long et al, 2015) pioneered end-to-end pixel-wise prediction, addressing the resolution loss issue inherent in traditional CNNs for segmentation tasks. Building upon this, U-Net (Ronneberger et al, 2015) introduced a symmetric encoder-decoder architecture with skip connections, enabling the fusion of low-level spatial and high-level semantic features. It has since become a benchmark in image segmentation. Subsequently, UNet++ (Zhou et al,

2018) constructed a nested U-shaped structure through dense skip connections, effectively mitigating the semantic gap caused by direct feature map concatenation. ResUNet++ (Jha et al, 2021) further incorporated residual connections and squeeze-and-excitation modules, alleviating gradient vanishing issues while enhancing the model’s responsiveness to critical feature channels. To better delineate ambiguous polyp boundaries, researchers have proposed various innovative solutions. PraNet (Fan et al, 2020) introduced a reverse attention mechanism that iteratively erases non-polyp regions to reinforce boundary detection. Its multi-stage refinement strategy significantly improved the model’s robustness in occluded scenarios. SANet (Hu et al, 2025) incorporated spatial attention and context refinement modules to enhance edge localisation and polyp boundary delineation, demonstrating the effectiveness of attention-guided feature learning in image segmentation. Similarly, boundary enhancement (Hu et al, 2025) and spatial attention modules (Fu et al, 2019) have been introduced to increase sensitivity to polyp edges. However, despite these improvements, CNN-based architectures are limited by local receptive fields and may fail to capture long-range contextual dependencies, motivating the exploration of attention and Transformer-based methods.

2.2 Light-weighted based Methods

To enable real-time colonoscopy polyp analysis, light-weighted network architectures have emerged as a key research focus. For example, UNeXt (Valanarasu and Patel, 2022) adopted a hybrid convolution-MLP architecture, reducing the parameter count by $72\times$ while increasing inference speed by $10\times$, thereby providing an efficient solution for real-time diagnostic scenarios. Similarly, MALUNet (Ruan et al, 2022) integrated multi-attention light-weighted modules, reducing parameters by $44\times$ compared to U-Net while maintaining an optimal balance between computational complexity and segmentation performance in skin lesion segmentation. These light-weighted designs typically employ techniques such as depthwise separable convolutions (Chollet, 2017), model pruning, and knowledge distillation to significantly reduce computational costs while preserving accuracy. Nevertheless, most existing light-weighted models struggle to preserve fine-grained boundary information, which is crucial for polyp segmentation tasks such as polyp detection.

2.3 Attention-based Methods

Recently, attention and Transformer-based architectures have gained traction in polyp segmentation due to their ability to capture global contextual dependencies. Vision Transformer (ViT) (Dosovitskiy et al, 2020) established global dependencies through self-attention mechanisms, though its direct application to segmentation has been limited by computational complexity and substantial data requirements. To address this, SETR (Zheng et al, 2021) utilised the Transformer as an encoder to extract global context while employing a progressively upsampling CNN decoder to recover details,

thus maintaining global modelling capability while improving detail restoration. Deformable DETR (Zhu et al, 2020) reduced computational complexity to a linear level by dynamically predicting attention offsets, offering a novel solution for real-time polyp detection. However, a persistent trade-off remains between model accuracy and computational efficiency: while Transformer-based models achieve superior accuracy, their heavy architectures hinder real-time deployment; conversely, light-weighted CNNs lack boundary precision due to limited representational capacity. Motivated by this challenge, our proposed MicroAUNet aims to achieve a new balance between efficiency and accuracy through boundary-enhanced multi-scale fusion, light-weighted convolutional design, and progressive knowledge distillation.

3 Our Method

3.1 Preliminary

Colonoscopy polyp segmentation networks are commonly built on an encoder–decoder architecture, where the encoder captures hierarchical semantics and the decoder restores spatial details. Classical U-Net and subsequent models, including UNet++, SANet, UNeXt, and MALUNet, have explored multi-scale fusion, attention, and light-weighted strategies, inspiring the design of our proposed MicroAUNet. It builds upon MALUNet by adopting depthwise separable dilated convolutions and a single-path, parameter-shared attention design to further enhance boundary perception and computational efficiency.

3.2 Boundary-Enhanced Multi-Scale Feature Fusion

To address the challenges of ambiguous polyp boundaries and morphological diversity, MicroAUNet incorporates a boundary-enhanced multi-scale feature fusion module. An overview of the proposed architecture is demonstrated in Figure 2. This design combines depthwise separable dilated convolutions with a shared channel–spatial attention mechanism, enabling efficient extraction of multi-scale contextual information while emphasising boundary regions.

Depthwise Separable Dilated Convolutions. Depthwise convolution applies filters independently to each channel, while depthwise separable convolution combines depthwise and pointwise (1×1) operations to decouple spatial and channel processing, thereby reducing parameters and computation with minimal accuracy loss. To further expand the receptive field without additional parameters, dilated convolution inserts spacing between kernel elements to achieve multi-scale contextual aggregation. To jointly leverage these advantages, MicroAUNet employs a depthwise separable dilated convolutional block, which decomposes convolution into two stages: dilated convolution for spatial sampling and pointwise convolution for channel fusion. This structure reduces parameter count from $K \times K \times C \times C$ to $K \times K \times C$, achieving efficient multi-scale feature extraction crucial for delineating small or morphologically diverse polyps.

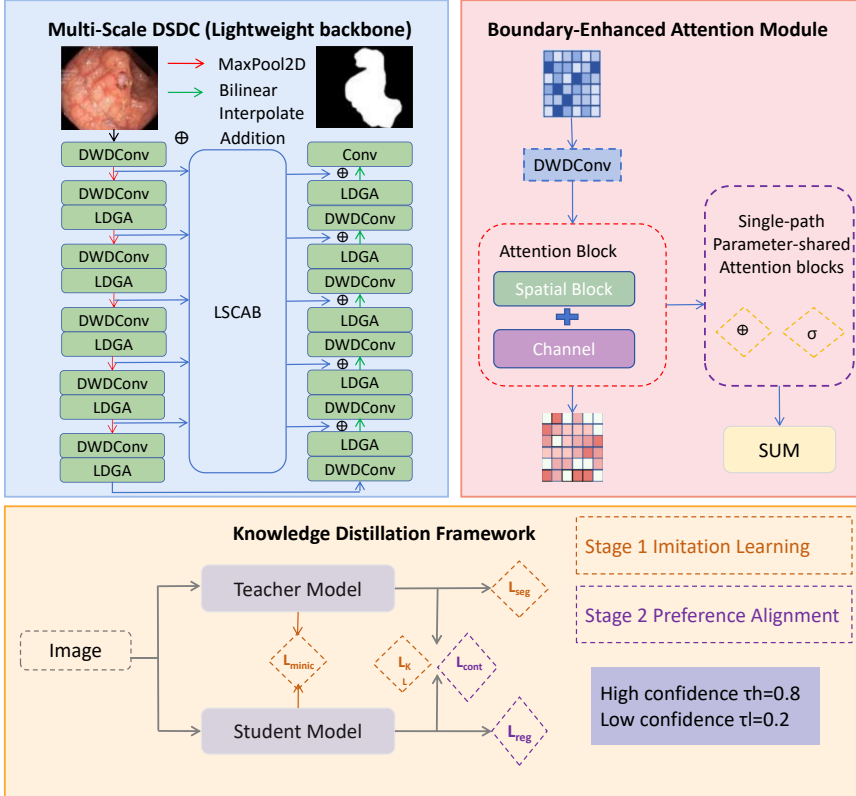


Fig. 2 Overview of the proposed MicroAUNet, which enhances boundary perception and achieves light-weighted segmentation through depthwise separable convolutions, shared attention, and progressive two-stage knowledge distillation.

Single-path and Parameter-shared Attention Block. Attention mechanisms are widely used to enhance feature discrimination by highlighting informative channels and salient spatial regions, enabling more accurate boundary localisation in complex endoscopic images. However, conventional multi-branch designs and independent parameterisation introduce excessive computational and memory overhead, limiting their applicability in light-weighted real-time systems. To overcome this limitation, MicroAUNet adopts a single-path spatial attention module and a parameter-shared channel–spatial attention bridge for efficient cross-scale feature integration. Specifically, the network includes two refinements: a single-path spatial attention mechanism for efficient saliency enhancement and a parameter-shared channel–spatial attention bridge for feature integration across decoder stages.

Multi-Scale Fusion Representation for Colonoscopy Polyp Image Segmentation

For spatial attention, a single-path depthwise separable convolution is employed to generate an attention mask:

$$A = \text{Sigmoid}(\mathbf{W}_{1 \times 1} \cdot \text{GELU}(\text{DWConv}(X))) \quad (1)$$

The attention weights are then applied to enhance salient features while retaining residual connections:

$$\mathbf{X}_{\text{out}} = \mathbf{A} \odot \mathbf{X} + \mathbf{X} \quad (2)$$

For cross-stage feature fusion, a parameter-shared spatial–channel attention bridge is introduced, which reuses shared fully connected layers across all decoder stages to minimise redundant parameters. The outputs of channel and spatial attention are then combined in a parallel weighted manner:

$$\mathbf{T}^{\text{out}} = (\alpha \cdot \mathbf{A}_c + \beta \cdot \mathbf{A}_s) \odot \mathbf{T} + \mathbf{T} \quad (3)$$

where \mathbf{A}_c and \mathbf{A}_s represent channel and spatial attention, respectively, and α, β are learning weights empirically initialized to 0.5. This parameter-sharing strategy promotes inter-stage feature consistency, enabling the model to simultaneously capture global semantics and fine-grained boundary details in complex endoscopic scenes.

3.3 Progressive Two-Stage Knowledge Distillation

Light-weighted networks typically suffer from degraded representation capacity due to limited parameters, particularly in modelling fine-grained semantics and boundaries. To address this challenge, a two-stage progressive knowledge distillation framework is introduced, where a high-capacity MALUNet serves as the teacher and MicroAUNet as the student. This framework enables the student to progressively absorb both semantic and boundary cues from the teacher during training.

Stage 1: Imitation Learning.

In the first stage (imitation learning), the Feature of the Student Network (F_S) aligns with the Feature of the Teacher Network (F_T) both at the feature and output distribution levels, where F_T^l and F_S^l denote the feature representations extracted from the l -th layer of the teacher and student networks, respectively. Feature-level alignment is enforced using an \mathcal{L}_2 mimicry loss:

$$\mathcal{L}_{\text{mimic}} = \sum_{l=1}^5 \lambda_l \|F_S^l - F_T^l\|_2^2 \quad (4)$$

while semantic consistency is maintained via KL divergence:

$$\mathcal{L}_{\text{KL}} = \frac{1}{N} \sum_{i=1}^N D_{\text{KL}}(T(x_i) \| S(x_i)) \quad (5)$$

Algorithm 1 Training procedure of MicroAUNet.

Input: Endoscopic image I ; Teacher model θ_T ; Student model θ_S ; Epochs N ;

Output: Optimized light-weighted model θ_S^{opt} ;

- 1: $F_0 \leftarrow$ Depthwise Separable Dilated Conv(I);
- 2: $F_1 \leftarrow$ LDGA(F_0); $F_2 \leftarrow$ LSCAB(F_1);
- 3: $F_e \leftarrow$ EncoderDecoderFusion(F_2);
- 4: **for** $t = 1$ to N **do** ▷ Imitation Learning
- 5: $\mathcal{L}_{mimic} = \sum_l \lambda_l * \|F_S^l - F_T^l\|_2^2$;
- 6: $\mathcal{L}_{KL} = \frac{1}{N} \sum_i D_{KL} * (T(x_i) \| S(x_i))$;
- 7: $\mathcal{L}_1 = \mathcal{L}_{seg} + (1 - \omega_{KL}) * \mathcal{L}_{mimic} + \omega_{KL} * \mathcal{L}_{KL}$; ▷ Preference Alignment
- 8: $\mathcal{L}_2 = \mathcal{L}_{seg} + \mathcal{L}_{cont} + \rho \mathcal{L}_{reg}$;
- 9: $\theta_S \leftarrow$ EMA(θ_S , \mathcal{L}_2);
- 10: **end for**
- 11: **return** θ_S^{opt} ▷ Final optimized MicroAUNet model

The overall loss integrates segmentation loss with distillation terms:

$$\mathcal{L}_1 = \mathcal{L}_{seg} + (1 - \omega_{KL}) \cdot \mathcal{L}_{mimic} + \omega_{KL} \cdot \mathcal{L}_{KL} \quad (6)$$

where the weighting factor ω_{KL} is dynamically adjusted during training, allowing a gradual transition from low-level features imitation to high-level semantic alignment. This stage allows the light-weighted model to capture rich semantic and boundary-aware representations from the teacher early in training.

Stage 2: Preference Alignment.

In the second stage, teacher predictions with high confidence ($\tau_h = 0.8$) are treated as positive samples, while low-confidence predictions ($\tau_l = 0.2$) are considered negative. A contrastive loss is employed to enhance intra-class compactness and inter-class separability, improving the student's decision boundary learning in complex scenarios. The final objective is defined as:

$$\mathcal{L}_2 = \mathcal{L}_{seg} + \mathcal{L}_{cont} + \rho \cdot \mathcal{L}_{reg} \quad (7)$$

where \mathcal{L}_{cont} encourages consistency among positive samples and differentiation from negatives, and \mathcal{L}_{reg} acts as a regularisation term to prevent overfitting, where ρ serves as a regularisation coefficient empirically set to 0.3 in this work. This two-stage progressive distillation framework enables MicroAUNet to achieve strong boundary delineation and semantic understanding despite its compact parameter space. A complete training procedure of MicroAUNet is illustrated in Algorithm 1.

4 Experiments

4.1 Datasets and Evaluation Metrics

To comprehensively evaluate the proposed MicroAUNet model, we conducted extensive experiments on two public polyp segmentation datasets: Kvasir-SEG (Jha et al, 2019) and CVC-ClinicDB (Bernal et al, 2015). All models were trained under the same hyperparameter settings outlined in Section 4.2 to ensure a fair comparison. The evaluation encompasses both comparative analysis against state-of-the-art methods and an internal ablation study to assess the individual contribution of each proposed component. Performance was evaluated using five standard metrics: mean Dice coefficient (mDice), mean Intersection over Union (mIoU), Accuracy (Acc), Specificity (Spe), and Sensitivity (Sen).

4.2 Implementation details

During the experiment, training was conducted for 300 epochs with a batch size of 8. The AdamW optimiser was employed with an initial learning rate of 0.001, and a cosine annealing learning rate scheduler was applied to improve training stability. To ensure reproducibility, the random seed was fixed at 42. All experiments were conducted on a platform equipped with an Intel(R) Xeon(R) Gold 6330 CPU @ 2.1 GHz with 128 GB of RAM and an NVIDIA GeForce RTX 3090 GPU with 24 GB of memory.

4.3 Comparison with State-of-the-Arts

To comprehensively evaluate the proposed MicroAUNet, experiments were conducted on the Kvasir-SEG and CVC-ClinicDB datasets, with comparisons against several representative segmentation models, including UNet, SANet, UNeXt, and MALUNet. The results are presented in Table 1 and visualised by radar charts in Figure 3.

The results demonstrate that MicroAUNet achieves the best trade-off between segmentation accuracy and efficiency, and generally outperforms other light-weighted and full-capacity models across both datasets. The baseline UNet performs significantly worse than the advanced architectures, achieving only 0.818/0.746 (mDice/mIoU) on Kvasir and 0.823/0.750 on CVC. While SANet and UNeXt exhibit moderate improvements through attention and MLP hybridisation, MicroAUNet attains the best trade-off between accuracy and efficiency. Specifically, MicroAUNet achieves 0.904/0.861 (mDice/mIoU) on Kvasir and 0.902/0.869 on CVC, surpassing MALUNet with substantially fewer parameters (0.0249M vs. 0.175M). MicroAUNet achieves a higher mDice score on Kvasir (0.904) than on CVC (0.902), whereas MALUNet performs better on CVC (mDice: 0.906). This difference may stem from the distinct characteristics of the two datasets: Kvasir encompasses diverse polyp morphologies, demanding stronger shape adaptability; CVC images have higher resolution, requiring more stringent detail preservation.

Table 1 Performance comparison of different models on Kvasir and CVC datasets, normalised scores are shown for Kvasir Dataset and CVC Dataset.

Model	Kvasir					CVC				
	mDice	mIoU	Acc	Spe	Sen	mDice	mIoU	Acc	Spe	Sen
UNet	0.818	0.746	0.940	0.967	0.859	0.823	0.750	0.953	0.966	0.860
SANet	0.886	0.847	0.944	0.960	0.895	0.898	0.869	0.957	0.963	0.901
UNExT	0.879	0.837	0.944	0.968	0.872	0.889	0.865	0.956	0.970	0.872
MALUNet	0.892	0.857	0.946	0.962	0.897	0.906	0.875	0.959	0.964	0.912
MicroAUNet	0.904	0.861	0.951	0.964	0.902	0.902	0.869	0.957	0.962	0.908

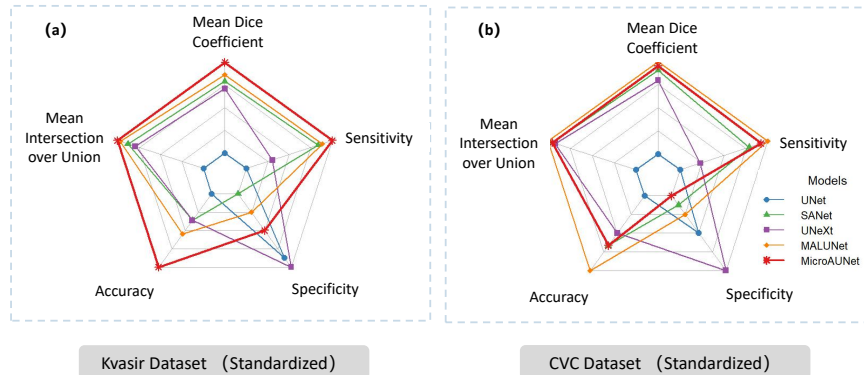


Fig. 3 Quantitative comparison of different segmentation models on Kvasir and CVC datasets. Radar charts visualise the performance (mDice, mIoU, Accuracy, Specificity, and Sensitivity) of UNet, SANet, UNExT, MALUNet, and the proposed MicroAUNet, demonstrating the superior accuracy–efficiency trade-off of MicroAUNet.

The model complexity analysis is presented in Table 2. MicroAUNet has only 0.0249M parameters, which is substantially fewer than UNet (7.77M) and SANet (23.90M). Although its GFLOPs (0.148) are slightly higher than MALUNet (0.083), MicroAUNet still maintains extremely low complexity while achieving superior segmentation accuracy. Figure 4 further supports these findings. These findings confirm the effectiveness of the proposed light-weighted architectural design, which trades off computational redundancy for improved efficiency while retaining robust representational capacity.

Removing the light-weighted strategy in MicroAUNet-1 led to a 1.34% decrease in mDice ($0.904 \rightarrow 0.892$) and a 0.47% drop in mIoU ($0.861 \rightarrow 0.857$) on the Kvasir dataset, demonstrating that the light-weighted module effectively improves segmentation accuracy through parameter compression and feature reuse. However, on the CVC dataset, MicroAUNet-1 slightly outperformed the full model in mDice (0.906 vs. 0.902). This may be attributed to the fact that lesions in the CVC dataset have clearer boundaries, where the

*Multi-Scale Fusion Representation for Colonoscopy Polyp Image Segmentation***Table 2** Comparison of Model complexity in terms of Params(M) and FLOPs (G).

Model	UNet	SANet	UNeXt	MALUNet	MicroAUNet
Params (M)	7.77	23.90	0.30	0.175	0.0249
FLOPs (G)	13.78	5.99	0.10	0.083	0.148

marginal feature loss from light-weighted convolution has a limited impact on segmentation performance.

In contrast, MicroAUNet-2, which excludes the imitation learning stage, exhibited a notable decline in performance. The mDice dropped by 3.21% (0.904 → 0.875) on Kvasir, and the mIoU decreased by 2.71% (0.869 → 0.846) on CVC. These results confirm that imitation learning via teacher–student knowledge distillation substantially enhances the model’s ability to distinguish subtle lesions in medical images.

When removing the preference contrastive learning mechanism (MicroAUNet-3), the mDice and mIoU decreased by 3.43% and 2.91%, respectively, on the Kvasir dataset. This indicates that the contrastive learning strategy strengthens intra-class feature consistency and improves robustness in complex backgrounds.

Overall, the proposed MicroAUNet achieves superior performance over all variants ablated across both data sets, reflecting the complementary and synergistic effects between the light-weighted design and the training strategy. The light-weighted modules reduce redundant parameters, while imitation and contrastive learning compensate for representational loss through feature-guided supervision. Consequently, the complete model achieves a maximum mDice of 0.904 on Kvasir and an mIoU of 0.869 on CVC, outperforming MicroAUNet-3 by 3.09%. Moreover, MicroAUNet exhibits the highest cross-dataset stability, with an mDice standard deviation of 0.0014 (0.904 vs. 0.902), which is notably lower than that of MicroAUNet-2 (0.0015) and MicroAUNet-3 (0.0040). These findings demonstrate that multi-component collaboration effectively enhances segmentation stability and robustness across datasets.

4.4 Ablation studies

To investigate the contributions of individual components, ablation studies were performed on the Kvasir and CVC-ClinicDB datasets, the results are shown in Table 3. Three variants were designed for comparison: MicroAUNet-1 (without depthwise separable dilated convolutions), MicroAUNet-2 (without the imitation learning stage), and MicroAUNet-3 (without the preference alignment stage).

4.5 Qualitative Analysis

Figure 5 shows qualitative comparisons among Ground Truth (GT), UNet, SANet, UNeXt, MALUNet, and the proposed MicroAUNet. As seen in

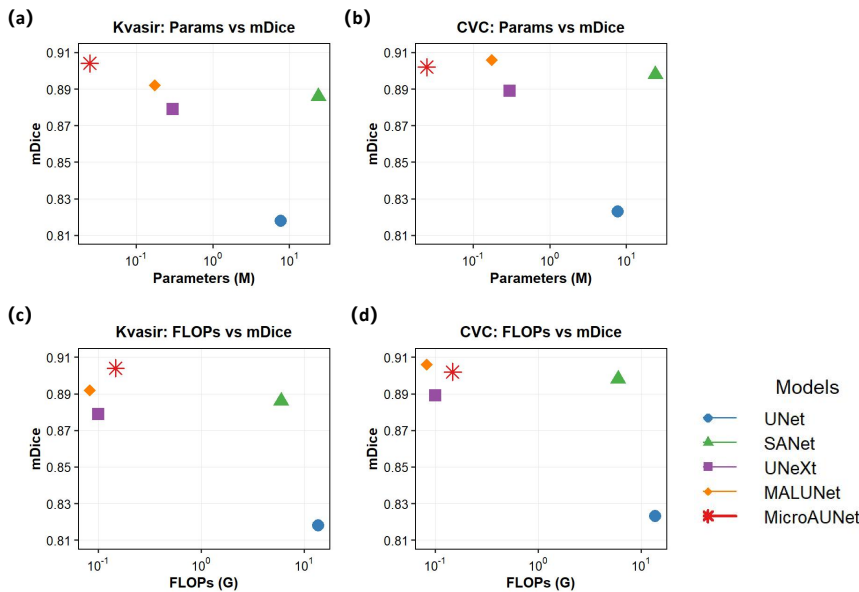


Fig. 4 Comprehensive analysis of efficiency and performance across models. Scatter plots compare parameter count and computational complexity (Params and FLOPs) versus segmentation accuracy, illustrating that MicroAUNet achieves the optimal balance among light-weighted and full-scale architectures.

Table 3 Ablation Study of proposed MicroAUNet method on the Kvasir and CVC-ClinicDB datasets.

Model	Kvasir						CVC					
	mDice	mIoU	Acc	Spe	Sen		mDice	mIoU	Acc	Spe	Sen	
MicroAUNet-1	0.892	0.857	0.946	0.960	0.896	0.906	0.875	0.960	0.966	0.911		
MicroAUNet-2	0.875	0.840	0.943	0.957	0.892	0.878	0.846	0.951	0.956	0.903		
MicroAUNet-3	0.873	0.836	0.941	0.955	0.891	0.881	0.843	0.953	0.959	0.906		
MicroAUNet	0.904	0.861	0.951	0.964	0.902	0.902	0.869	0.957	0.962	0.908		

the first two models, U-Net and SANet miss part of the polyp edges or produce fragmented masks. UNeXt and MALUNet generate more complete results but still blur fine boundaries in low-contrast areas. In contrast, MicroAUNet accurately delineates polyp contours and maintains boundary continuity, even under occlusion or irregular shapes. The red circles highlight that MicroAUNet removes background artefacts and better preserves small structures, demonstrating clearer and more reliable segmentation consistent with the ground truth.

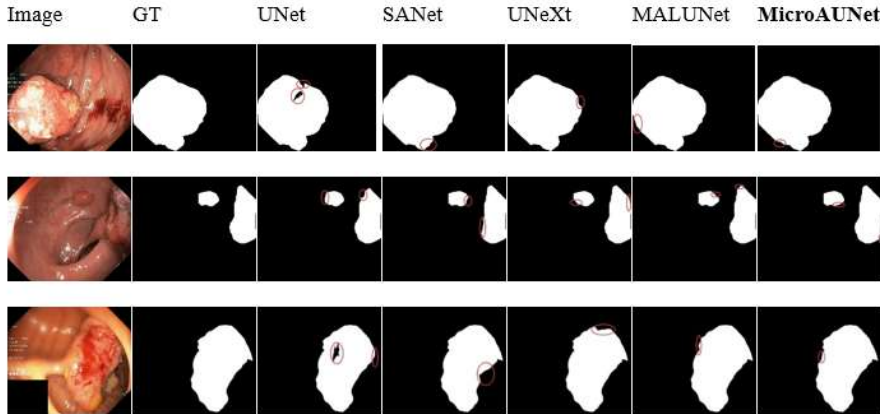
Multi-Scale Fusion Representation for Colonoscopy Polyp Image Segmentation

Fig. 5 Visual comparison between the proposed method and four state-of-the-art ones. Visual examples show that MicroAUNet produces sharper, more continuous boundaries and fewer background artefacts compared with UNet, SANet, UNeXt, and MALUNet, yielding results closest to the ground truth.

4.6 Discussion and Limitation

The proposed MicroAUNet achieves an effective balance between segmentation precision and computational efficiency, making it well-suited for real-time clinical applications. Conventional segmentation networks often rely on heavy backbones or complex attention mechanisms, which increase the number of parameters and latency. In contrast, MicroAUNet employs depthwise separable dilated convolutions and a parameter-shared single-path attention design, enabling efficient multi-scale boundary extraction with minimal redundancy.

While light-weighted models typically risk losing representational capacity, the introduced progressive two-stage knowledge distillation successfully transfers both semantic and boundary knowledge from a teacher model, preserving high segmentation accuracy under a limited number of parameters. Visualisation results further indicate that MicroAUNet captures clearer boundary activations than existing light-weighted methods. Experiments on Kvasir and CVC-ClinicDB demonstrate that MicroAUNet surpasses state-of-the-art models in mDice and mIoU while using fewer parameters and achieving faster inference. Nonetheless, its performance may decline on extremely low-quality or unseen imaging styles.

Although MicroAUNet achieves a favourable balance between accuracy and efficiency, some limitations remain. Its generalisation to unseen clinical environments, such as images from different endoscopic devices or lighting conditions, has not been fully validated. While strong performance is shown on Kvasir and CVC-ClinicDB, evaluation on multi-centre or real-world datasets is needed to confirm broader robustness. Additionally, the two-stage distillation framework relies on the teacher model's quality; biased or noisy teacher

representations may limit the student network's performance. Future work will investigate self-distillation or teacher-free strategies to improve adaptability.

5 Conclusion

In this work, we proposed MicroAUNet, a boundary-enhanced light-weighted segmentation model that achieves both high accuracy and real-time efficiency. The model integrates a boundary-enhanced multi-scale fusion module for precise edge localisation and a progressive two-stage knowledge distillation strategy for robust light-weighted learning. Comprehensive experiments verify that MicroAUNet achieves state-of-the-art segmentation performance with substantially reduced computational cost, demonstrating strong potential for real-time colonoscopic deployment. Future research will focus on exploring domain adaptation and contrastive learning to enhance cross-domain generalisation across diverse imaging devices and clinical conditions.

Acknowledgments. This work was partially supported by the National Natural Science Foundation of China under Grant No.62301315, Startup Fund for Young Faculty at SJTU (SFYF at SJTU) under Grant No.23X010501967, Shanghai Municipal Health Commission Health Industry Clinical Research Special Project under Grant No.202340010 and 2025 Key Research Initiatives of Yunnan Erhai Lake National Ecosystem Field Observation Station under Grant No.2025ZD03. The authors would like to thank the anonymous reviewers for their valuable suggestions and constructive criticisms.

Declarations

- **Funding**

This work was partially supported by the National Natural Science Foundation of China under Grant No.62301315, Startup Fund for Young Faculty at SJTU (SFYF at SJTU) under Grant No.23X010501967, Shanghai Municipal Health Commission Health Industry Clinical Research Special Project under Grant No.202340010 and 2025 Key Research Initiatives of Yunnan Erhai Lake National Ecosystem Field Observation Station under Grant No.2025ZD03.

- **Conflict of interest**

The authors declare that they have no conflict of interest.

- **Ethics approval**

Not Applicable. The datasets and the work do not contain personal or sensitive information, no ethical issue is concerned.

- **Consent to participate**

The authors are fine that the work is submitted and published by Machine Learning Journal. There is no human study in this work, so this aspect is not applicable.

- **Consent for publication**

The authors are fine that the work (including all content, data and images) is published by Machine Learning Journal.

- **Availability of data and material**

The data used for the experiments in this paper are available online, see Section 4.1 for more details.

- **Code availability**

The code is publicly available at <https://github.com/JeremyXSC/MicroAUNet>.

- **Authors' contributions**

Ziyi Wang, Yuanmei Zhang, Suncheng Xiang contributed conception and design of the study, as well as the experimental process and interpreted model results. Suncheng Xiang obtained funding for the project and provided clinical guidance. Ziyi Wang and Yuanmei Zhang drafted the manuscript. All authors contributed to manuscript revision, read and approved the submitted version.

References

Akgöl Y, Toptaş B, Toptaş M (2025) Polyp segmentation with colonoscopic images: a study. *Neural Computing and Applications* pp 1–36

Bernal J, Sánchez FJ, Fernández-Esparrach G, et al (2015) Wm-dova maps for accurate polyp highlighting in colonoscopy: Validation vs. saliency maps from physicians. *Computerized medical imaging and graphics* 43:99–111

Chollet F (2017) Xception: Deep learning with depthwise separable convolutions. In: Proceedings of the IEEE conference on computer vision and pattern recognition, pp 1251–1258

Dosovitskiy A, Beyer L, Kolesnikov A, et al (2020) An image is worth 16x16 words: Transformers for image recognition at scale. *arXiv preprint arXiv:201011929*

Fan DP, Ji GP, Zhou T, et al (2020) Pranet: Parallel reverse attention network for polyp segmentation. In: International conference on medical image computing and computer-assisted intervention, Springer, pp 263–273

Fu J, Liu J, Tian H, et al (2019) Dual attention network for scene segmentation. In: Proceedings of the IEEE/CVF conference on computer vision and pattern recognition, pp 3146–3154

Hu BC, Ji GP, Shao D, et al (2025) Pranet-v2: Dual-supervised reverse attention for medical image segmentation. *arXiv preprint arXiv:250410986*

Jha D, Smedsrød PH, Riegler MA, et al (2019) Kvasir-seg: A segmented polyp dataset. In: International conference on multimedia modeling, Springer, pp

Jha D, Smedsrud PH, Johansen D, et al (2021) A comprehensive study on colorectal polyp segmentation with resunet++, conditional random field and test-time augmentation. *IEEE journal of biomedical and health informatics* 25(6):2029–2040

Long J, Shelhamer E, Darrell T (2015) Fully convolutional networks for semantic segmentation. In: *Proceedings of the IEEE conference on computer vision and pattern recognition*, pp 3431–3440

Mei J, Zhou T, Huang K, et al (2025) A survey on deep learning for polyp segmentation: Techniques, challenges and future trends. *Visual Intelligence* 3(1):1

Qayoom A, Xie J, Ali H (2025) Polyp segmentation in medical imaging: challenges, approaches and future directions. *Artificial Intelligence Review* 58(6):169

Ronneberger O, Fischer P, Brox T (2015) U-net: Convolutional networks for biomedical image segmentation. In: *International Conference on Medical image computing and computer-assisted intervention*, Springer, pp 234–241

Ruan J, Xiang S, Xie M, et al (2022) Malunet: A multi-attention and light-weight unet for skin lesion segmentation. In: *2022 IEEE International Conference on Bioinformatics and Biomedicine (BIBM)*, IEEE, pp 1150–1156

Sabri O, Abouelmehdi K, et al (2025) Advanced polyp segmentation using u-net architecture: A review. *Practical Applications of Machine Learning and AI: Medicine, Environmental Science, Transportation, and Education* pp 91–116

Si C, Rahim MSM, Mianzhou Y, et al (2023) Unet-based polyp segmentation: A survey. In: *2023 IEEE International Conference on Computing (ICOCO)*, IEEE, pp 154–159

Valanarasu JMJ, Patel VM (2022) Unext: Mlp-based rapid medical image segmentation network. In: *International conference on medical image computing and computer-assisted intervention*, Springer, pp 23–33

Zheng S, Lu J, Zhao H, et al (2021) Rethinking semantic segmentation from a sequence-to-sequence perspective with transformers. In: *Proceedings of the IEEE/CVF conference on computer vision and pattern recognition*, pp 6881–6890

Zhou Z, Rahman Siddiquee MM, Tajbakhsh N, et al (2018) Unet++: A nested u-net architecture for medical image segmentation. In: International workshop on deep learning in medical image analysis, Springer, pp 3–11

Zhu X, Su W, Lu L, et al (2020) Deformable detr: Deformable transformers for end-to-end object detection. arXiv preprint arXiv:201004159